Phase Diagram Data for Several PEG + Salt Aqueous Biphasic Systems at 25 °C

Jonathan G. Huddleston,* Heather D. Willauer, and Robin D. Rogers

Center for Green Manufacturing and Department of Chemistry, The University of Alabama, Tuscaloosa, Alabama 35487

Phase diagrams determined by the cloud point method at 25 °C, including tie lines assigned from mass phase ratios according to the lever arm rule, are presented for several poly(ethylene glycol) (PEG) + salt aqueous biphasic systems (ABS). The systems include PEG-1000 + K_3PO_4, PEG-2000 + K_3PO_4, PEG-3400 + K_3PO_4, and PEG-2000 in combination with the following salts K_2CO_3, $(NH_4)_2SO_4$, Li_2SO_4, $ZnSO_4$, $MnSO_4$, and NaOH.

Introduction

Aqueous biphasic systems (ABS), also known as aqueous two-phase systems, have been applied for over 40 years to the separation, fractionation, and molecular characterization of biological macromolecules and particles.[1−5] Applications to protein purification at industrial scales have been discussed in the literature over the last 25 years.[6,7] Despite strong efforts to improve adsorption steps in industrial bioprocessing, ABS are still seen to have considerable advantages in the early stages of biorecovery processes, especially with regard to efficient throughput and space−time yield.[8] During the same time frame, applications of ABS to biotransformations have also been the subject of some interest.[9,10] In more recent years, increasingly diverse applications of ABS have appeared in the literature. These include applications to the recovery of metal ions and radiochemicals;[11−13] applications in the recovery of dyes, drug molecules, and small organic species;[14−17] and applications to the recovery of inorganic particles.[18] A yet more recent emerging trend has been the investigation of ABS as an alternative solvent system for chemical reactions. Processes employing ABS have been demonstrated in the recovery of lignin and cellulose during paper pulping.[19,20] Aqueous biphasic reactive extraction (ABRE) processes employing alkaline earth metal catalysts for delignification in paper pulping have been demonstrated.[21] Most recently, an ABRE process was demonstrated for the conversion of cyclohexene to adipic acid in a reaction employing hydrogen peroxide and a tungstate catalyst.[22] These latest developments suggest the opening of a new phase in the development of applied ABS processes.

Undoubtedly, commercial applications of ABS have been slow to develop, for which a number of reasons may be adduced. Development of processes still appears to be heuristic, and there are currently no suppliers of specific applications or products, as is ubiquitously found for adsorption processes. Recycling of phases is perceived as far more problematic than that for aqueous + organic systems. On the other hand, chemical and water usage is beginning to seem more problematic in process chromatography steps as well.[23]

By now there is considerable data in the literature relating to the operation of ABS, including phase diagrams, their physical chemistry, and the purification of particular products. We present here some phase diagrams of PEG + salt ABS that have not been previously published. Some other sources of phase diagram data for ABS should, perhaps, be mentioned here. Albertsson's seminal monograph is, of course, well-known.[1] The book by Zaslavsky contains a summary of most of the phase diagram data available at that time.[4] Considerable new and useful phase diagram data have appeared in the literature since including, but not comprehensively, data relating to PEG + salt systems,[24−27] to PEG + dextran systems,[28−30] and to systems employing copolymers.[31,32]

Methods

The salts $(NH_4)_2SO_4$, K_3PO_4, K_2CO_3, Li_2SO_4, $MnSO_4$, NaOH, and $ZnSO_4$ and the polymers PEG-1000, PEG-2000, and PEG-3400 used were obtained from Aldrich (Milwaukee, WI) and were of reagent grade. Water was obtained from a commercial deionization system (Barnsted, Dubuque, IA). For the preparation of phase diagrams, stock solutions of polymer and salt were prepared on a mass percent basis. Phase diagrams were determined by the cloud point method[33] and fitted by least squares regression to an empirical relationship developed by Merchuk[34] and shown in eq 1. Measurements of mass for the preparation of stock solutions and for the determination of cloud points were made in grams on a top loading balance to four significant figures. Compositions were then calculated and reduced to two significant figures prior to the fitting of binodals and tie lines.

$$Y_A = a\exp(bX_A^{0.5} - cX_A^{3}) \tag{1}$$

where Y_A and X_A are the concentrations of polymer and salt, respectively, which had been determined to lie on the cloud point curve. Tie lines for each ABS were assigned by application of the lever arm rule to the relationship between the mass phase composition and the overall

* Corresponding author. Fax: (205) 348-0823. E-mail: jhuddles@bama.ua.edu.

10.1021/je034042p CCC: $25.00
Published on Web 07/23/2003

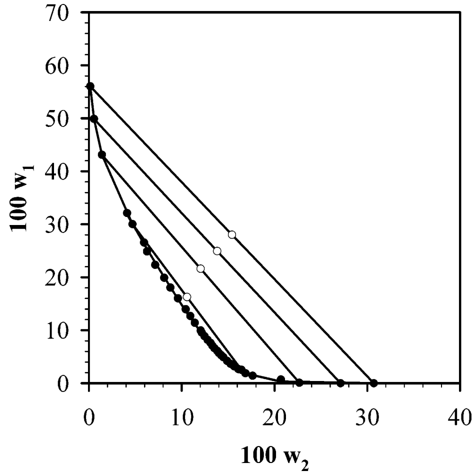

Figure 1. Phase diagram in w/w % of the PEG-1000 (1) + K_3PO_4 (2) ABS, showing the binodal curve determined by cloud point titration (●), the fitted cloud point curve, and the overall and node compositions (○) of several fitted tie lines.

Table 1. Empirical Coefficients of Eq 1 for Various PEG + Salt ABS

system	*a*	*b*	*c*	r^2
1 K_3PO_4/PEG-1000	63.40	−0.3242	4.285×10^{-4}	0.9998
2 K_3PO_4/PEG-2000	115.88	−0.6685	5.727×10^{-4}	0.9992
3 K_3PO_4/PEG-3400	77.35	−0.5213	1.141×10^{-3}	0.9998
4 K_2CO_3/PEG-2000	124.20	−0.5589	9.392×10^{-4}	0.9991
5 $(NH_4)_2SO_4$/PEG-2000	87.41	−0.4360	4.303×10^{-4}	0.9988
6 Li_2SO_4/PEG-2000	73.98	−0.3444	6.590×10^{-4}	0.9996
7 $MnSO_4$/PEG-2000	65.65	−0.4293	2.671×10^{-4}	0.9997
8 $ZnSO_4$/PEG-2000	70.69	−0.4542	$2.970 \times 10^{-}_{4}$	0.9918
9 NaOH/PEG-2000	105.79	−0.5572	2.346×10^{-3}	0.9990

system composition. Details of the mathematical methods used are given elsewhere.[15,34] The phase relationships were also placed on a molal basis by conversion of the mass percent data (data not shown).

Cloud point data for systems composed of different salt types were also fitted to the statistical geometrical relationship of Lilley[35] shown in eq 2:

$$w_1 = -\ln\left(V^* \frac{w_2}{M_2}\right)\frac{M_1}{V^*} \tag{2}$$

where w_1 is the salt concentration, w_2 is the polymer concentration, M_2 and M_1 are the polymer and salt molar masses, and V^* is the scaled excluded volume. As noted by Lilley, because of the variation in the density along the cloud point curve, this is an empirical application of the statistical geometry approach. The interest lies in the behavior of the single fitted parameter of eq 2 in systems formed with a variety of different salts.

Results

Phase diagrams for the various PEG + salt systems examined here are shown in Figures 1−9. The binodal curves have been fitted according to the empirical relationship of Merchuk,[34] and the coefficients for this regression as determined by least squares regression of the cloud point data are shown in Table 1. The raw cloud point data (to two significant figures) for these systems are given in Table 2 so that fitting by other mathematical or thermodynamic relationships is enabled. While Figures 1−9 and the regression coefficients in Table 1 indicate that the empirical equation (eq 1) gives a rather good fit to the data for

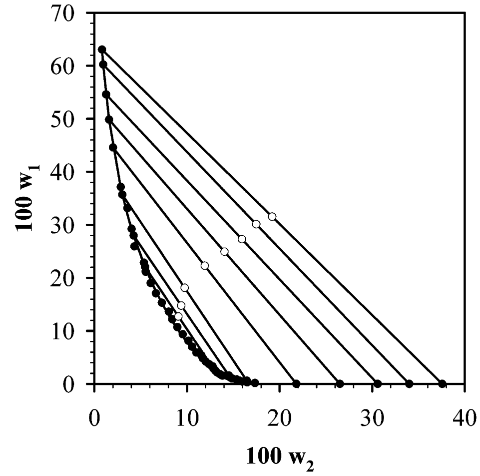

Figure 2. Phase diagram in w/w % of the PEG-2000 (1) + K_3PO_4 (2) ABS, showing the binodal curve determined by cloud point titration (●), the fitted cloud point curve, and the overall and node compositions (○) of several fitted tie lines.

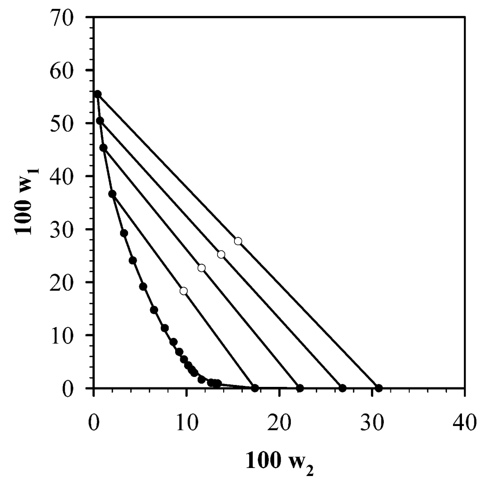

Figure 3. Phase diagram in w/w % of the PEG-3400 (1) + K_3PO_4 (2) ABS, showing the binodal curve determined by cloud point titration (●), the fitted cloud point curve, and the overall and node compositions (○) of several fitted tie lines.

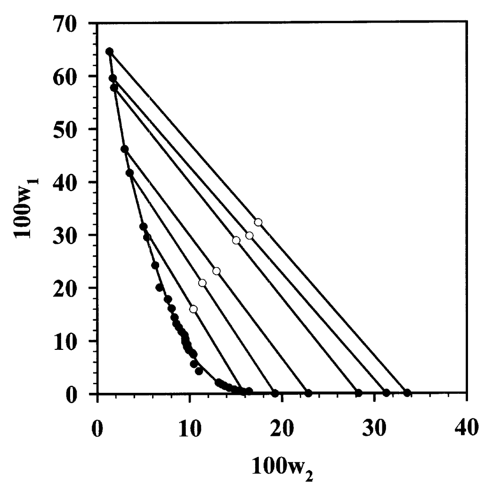

Figure 4. Phase diagram in w/w % of the PEG-2000 (1) + K_2CO_3 (2) ABS, showing the binodal curve determined by cloud point titration (●), the fitted cloud point curve, and the overall and node compositions (○) of several fitted tie lines.

descriptive purposes, it is in many ways deficient. The exact form of the data and, perhaps, the way it has been collected

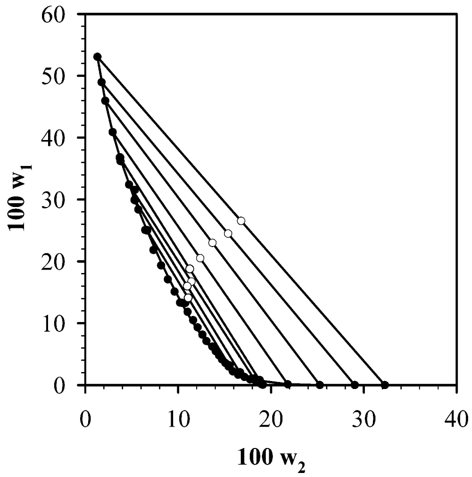

Figure 5. Phase diagram in w/w % of the PEG-2000 (1) + $(NH_4)_2SO_4$ (2) ABS, showing the binodal curve determined by cloud point titration (●), the fitted cloud point curve, and the overall and node compositions (○) of several fitted tie lines.

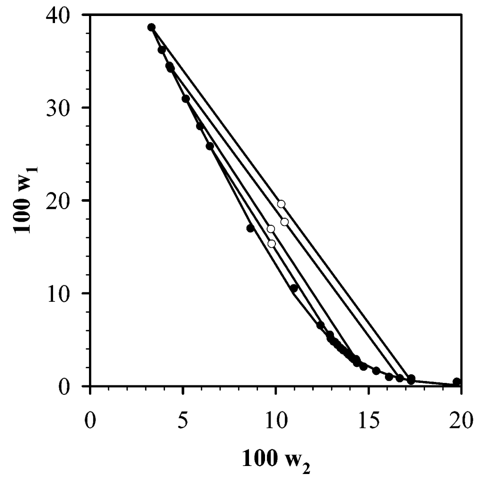

Figure 6. Phase diagram in w/w % of the PEG-2000 (1) + Li_2SO_4 (2) ABS, showing the binodal curve determined by cloud point titration (●), the fitted cloud point curve, and the overall and node compositions (○) of several fitted tie lines.

result in an interplay between the various coefficients such that there is little systematic variation which could be used in deriving a general description of a PEG + salt binodal curve which was independent of salt type and polymer molecular weight.

Tie lines for these cloud point curves were fitted by a least-squares method based on the lever arm rule described previously,[15] and these are shown in Figures 1−9. Numerical data for these tie lines are given in Table 3. The average slope of the tie lines is also shown in Table 3. As may be seen from these data and from Figures 1−9, the slope of the tie lines is approximately constant at short tie line lengths but there is significant change in tie line slope as tie line length increases. This is probably due to the fact

Table 2. Experimentally Determined Cloud Points for PEG (1) + Salt (2) + Water (3)

PEG-1000 + K_3PO_4		PEG-2000 + K_3PO_4		PEG-3400 + K_3PO_4		PEG-2000 + K_2CO_3		PEG-2000 + $(NH_4)_2SO_4$		PEG-2000 + Li_2SO_4		PEG-2000 + $MnSO_4$		PEG-2000 + $ZnSO_4$		PEG-2000 + NaOH	
$100w_2$	$100w_1$	$100w_2$	$100w_1$	$100w_2$	$100w_1$	$100w_2$	$100w_1$	$100w_2$	$100w_1$	$100w_2$	$100w_1$	$100w_2$	$100w_1$	$100w_2$	$100w_1$	$100w_2$	$100w_1$
4.12	32.12	2.85	37.15	3.27	29.23	5.44	29.52	3.79	36.21	4.34	34.20	3.96	27.74	1.85	37.53	2.39	43.92
5.94	26.55	3.56	33.15	4.21	24.09	6.28	24.23	5.35	31.56	5.93	28.00	5.25	23.35	4.60	29.52	3.33	34.27
6.26	24.88	4.03	29.26	5.33	19.18	6.75	20.03	5.71	28.39	8.64	17.00	7.30	18.20	4.75	23.86	4.41	26.02
7.15	22.34	4.32	25.93	6.50	14.76	7.65	17.82	6.45	25.08	10.97	10.53	9.03	14.82	6.64	18.95	5.59	18.99
8.12	19.89	5.35	22.89	7.66	11.35	8.06	16.08	7.34	21.83	12.41	6.56	10.49	12.18	8.05	15.69	6.45	14.32
8.78	18.05	5.54	21.16	8.60	8.73	8.37	14.39	8.16	19.35	12.91	5.54	11.07	11.16	10.80	11.23	6.70	12.96
9.60	16.03	6.08	19.02	9.22	6.86	8.57	13.22	8.89	17.09	12.96	5.12	11.76	9.95	12.06	8.80	6.90	11.86
10.44	13.96	6.64	17.09	9.73	5.44	8.84	12.52	9.62	15.11	13.19	4.74	12.57	8.55	13.41	6.77	7.14	10.67
10.93	12.69	7.28	15.32	10.18	4.32	9.14	11.70	10.20	13.33	13.32	4.45	13.00	7.86	14.48	5.03	7.37	9.51
11.41	11.40	8.04	13.63	10.56	3.52	9.44	11.11	10.78	13.29	13.49	4.11	13.51	7.04	15.84	3.60	7.59	8.41
12.05	9.96	8.41	12.20	10.60	3.39	9.53	10.41	10.45	13.28	13.63	3.87	13.85	6.54	17.20	2.52	7.88	7.04
12.17	9.55	8.96	10.72	10.84	2.90	9.54	9.96	11.02	11.84	13.84	3.57	14.19	6.06	18.05	1.82	8.04	6.30
12.47	8.87	9.54	9.37	11.62	1.63	9.57	9.64	11.61	10.50	13.92	3.40	14.59	5.53	21.56	0.30	8.23	5.46
12.79	8.19	10.15	8.14	12.66	1.05	9.76	9.32	12.10	9.33	14.04	3.21	14.89	5.11			8.38	4.80
13.11	7.60	10.54	7.04	13.06	0.96	9.77	9.06	12.61	8.16	14.12	3.04	15.37	4.51			8.96	2.79
13.31	7.10	11.01	5.93	13.38	0.91	9.74	8.80	13.04	7.12	14.19	2.92	15.84	4.06			9.35	2.00
13.54	6.62	11.30	5.92			9.81	8.63	13.68	6.22	14.36	2.72	16.92	2.95			10.07	1.04
13.83	6.11	11.55	5.40			9.90	8.41	14.04	5.49	14.37	2.50	17.94	2.08			10.77	0.71
14.01	5.70	11.70	4.87			9.94	8.21	14.40	4.81	14.73	2.10	18.18	2.10				
14.26	5.29	12.02	4.23			10.31	7.70	14.72	4.15	15.41	1.64	19.36	1.38				
14.50	4.91	12.38	3.75			10.41	7.40	15.09	3.57	16.10	1.00	19.73	1.24				
14.89	4.22	12.77	3.31			10.47	5.59	15.44	2.99	17.30	0.84	21.27	0.87				
15.27	3.67	12.86	2.91			11.01	4.24	15.88	2.23	19.75	0.48	22.14	0.48				
15.65	3.19	13.06	2.53			13.15	2.10	16.47	1.67								
16.17	2.67	13.24	2.18			13.43	1.81	17.13	1.31								
16.87	1.90	13.54	1.85			13.77	1.48	17.74	0.93								
17.64	1.42	13.80	1.58			14.25	1.15	18.39	0.59								
20.69	0.701	14.26	1.59			14.83	0.80	18.75	0.35								
		14.54	1.38			15.42	0.59	18.98	0.14								
		14.67	1.22			16.42	0.42	19.13	0.05								
		14.88	1.03					21.80	0.13								
		15.39	0.85														
		15.39	0.72														
		15.68	0.61														
		15.98	0.46														
		16.50	0.32														
		17.34	0.18														

Table 3. Tie Line Compositions of PEG (1) + Salt (2) + Water (3) Assigned by the Lever Arm Rule

PEG-1000 (1) + K_3PO_4 (2) + Water (3)

	tie 1	tie 2	tie 3	tie 4
$100w_1$(mixture)	18.96	18.32	17.73	17.17
$100w_2$(mixture)	9.43	13.66	17.62	21.34
$100w_1$(top)	30.02	43.12	49.88	56.04
$100w_1$(bottom)	2.54	0.09	2.84×10^{-3}	4.33×10^{-5}
$100w_2$(top)	4.70	1.40	0.55	0.14
$100w_2$(bottom)	16.44	22.68	27.11	30.70
phase ratio (mass)	0.598	0.424	0.353	0.31
tie line length	29.89	48.00	56.52	63.83
tie line slope	−2.34	−2.02	−1.88	−1.83

PEG-2000 (1) + K_3PO_4 (2) + Water (3)

	tie 1	tie 2	tie 3	tie 4	tie 5	tie 6
$100w_1$(mixture)	18.88	18.24	17.60	17.09	16.56	16.36
$100w_2$(mixture)	9.46	13.72	17.69	21.41	24.91	28.20
$100w_1$(top)	35.69	44.58	49.85	54.60	60.23	63.06
$100w_1$(bottom)	0.59	0.013	8.54×10^{-5}	2.16×10^{-7}	3.98×10^{-10}	1.25×10^{-13}
$100w_2$(top)	3.02	2.022	1.58	1.26	0.96	0.83
$100w_2$(bottom)	16.47	21.81	26.52	30.60	33.99	37.57
phase ratio (mass)	0.521	0.409	0.354	0.313	0.275	0.255
tie line length	37.58	48.76	55.73	61.98	68.70	72.98
tie line slope	−2.61	−2.25	−2.00	−1.86	−1.82	−1.72

PEG-3400 (1) + K_3PO_4 (2) + Water (3)

	tie 1	tie 2	tie 3	tie 4
$100w_1$(mixture)	18.97	18.33	17.74	17.18
$100w_2$(mixture)	9.42	13.66	17.62	21.33
$100w_1$(top)	36.64	45.35	50.44	55.45
$100w_1$(bottom)	0.02	2.44×10^{-5}	1.48×10^{-9}	1.85×10^{-14}
$100w_2$(top)	2.00	1.04	0.67	0.41
$100w_2$(bottom)	17.37	22.22	26.81	30.72
phase ratio (mass)	0.517	0.404	0.352	0.310
tie line length	39.71	50.05	56.81	63.19
tie line slope	−2.38	−2.14	−1.93	−1.83

PEG-2000 (1) + K_2CO_3 (2) + Water (3)

	tie 1	tie 2	tie 3	tie 4	tie 5	tie 6
$100w_1$(mixture)	19.07	18.70	18.35	17.68	17.34	17.05
$100w_2$(mixture)	9.34	12.21	14.97	20.19	22.67	25.05
$100w_1$(top)	31.57	41.73	46.22	57.76	59.59	64.59
$100w_1$(bottom)	0.33	0.01	1.14×10^{-4}	3.78×10^{-9}	1.77×10^{-12}	1.98×10^{-15}
$100w_2$(top)	5.01	3.53	2.97	1.85	1.70	1.36
$100w_2$(bottom)	15.82	19.25	22.87	28.28	31.28	33.54
phase ratio (mass)	0.600	0.448	0.397	0.306	0.291	0.264
tie line length	33.06	44.58	50.31	63.53	66.53	72.168
tie line slope	−2.89	−2.65	−2.32	−2.18	−2.01	−2.01

PEG-2000 (1) + $(NH_4)_2SO_4$ (2) + Water (3)

	tie 1	tie 2	tie 3	tie 4	tie 5
$100w_1$(mixture)	19.55	19.29	19.17	18.80	18.57
$100w_2$(mixture)	10.23	12.94	15.62	18.55	21.43
$100w_1$(top)	32.41	40.90	46.00	48.97	53.07
$100w_1$(bottom)	1.04	0.13	9.52×10^{-3}	2.27×10^{-4}	3.91×10^{-6}
$100w_2$(top)	4.72	2.95	2.14	1.75	1.30
$100w_2$(bottom)	18.15	21.81	25.26	29.02	32.26
phase ratio (mass)	0.590	0.470	0.417	0.384	0.350
tie line length	34.12	44.92	51.44	56.04	61.44
tie line slope	−2.33	−2.16	−1.99	−1.80	−1.71

PEG-2000 (1) + Li_2SO_4 (2) + Water (3)

	tie 1	tie 2	tie 3	tie 4
$100w_1$(mixture)	19.31	19.22	19.13	19.00
$100w_2$(mixture)	8.53	8.98	9.93	10.52
$100w_1$(top)	25.84	30.94	34.50	38.64
$100w_1$(bottom)	4.82	2.90	0.85	0.59
$100w_2$(top)	6.45	5.15	4.27	3.30
$100w_2$(bottom)	13.11	14.32	16.68	17.29
phase ratio (mass)	0.690	0.582	0.543	0.484
tie line length	22.05	29.50	35.86	40.54
tie line slope	−3.16	−3.06	2.71	−2.72

Table 3. (Continued)

PEG-2000 (1) + $MnSO_4$ (2) + Water (3)

	tie 1	tie 2	tie 3	tie 4	tie 5
$100w_1$(mixture)	18.93	18.78	18.67	18.53	18.45
$100w_2$(mixture)	9.38	9.85	10.92	11.36	12.01
$100w_1$(top)	29.09	30.70	33.33	34.67	36.43
$100w_1$(bottom)	1.32	1.21	0.69	0.62	0.48
$100w_2$(top)	3.49	3.07	2.46	2.19	1.87
$100w_2$(bottom)	19.58	19.84	21.30	21.54	22.14
phase ratio (mass)	0.634	0.596	0.551	0.526	0.500
tie line length	32.09	33.92	37.68	39.16	41.27
tie line slope	−1.73	−1.76	−1.73	−1.76	−1.77

PEG-2000 (1) + $ZnSO_4$ (2) + Water (3)

	tie 1	tie 2	tie 3	tie 4
$100w_1$(mixture)	18.31	18.25	18.05	18.00
$100w_2$(mixture)	11.87	12.52	13.07	13.72
$100w_1$(top)	35.54	37.76	39.19	39.98
$100w_1$(bottom)	0.38	0.31	0.26	0.16
$100w_2$(top)	2.27	1.89	1.68	1.57
$100w_2$(bottom)	21.86	22.29	22.66	23.59
phase ratio (mass)	0.510	0.479	0.457	0.448
tie line length	40.26	42.65	44.23	45.51
tie line slope	−1.79	−1.84	−1.85	−1.81

PEG-2000 (1) + NaOH (2) + Water (3)

	tie 1	tie 2	tie 3
$100w_1$(mixture)	19.25	18.96	18.68
$100w_2$(mixture)	7.27	8.95	10.58
$100w_1$(top)	40.92	49.41	54.45
$100w_1$(bottom)	0.57	0.050	2.32e-3
$100w_2$(top)	2.65	1.80	1.39
$100w_2$(bottom)	11.26	13.39	15.38
mass ratio	0.463	0.383	0.343
tie line length	41.26	50.71	56.21
tie line slope	−4.68	−4.26	−3.89

Table 4. Effective Excluded Volume As Determined by Regression of Lilley's Statistical Geometry Model on the PEG + Salt ABS

salt system	apparent scaled EEV × 10^6 (kg/mol)	molar mass (g/mol)	regression coefficient, r^2
$ZnSO_4$	31.73	161.46	0.92
K_3PO_4	48.40	212.27	0.93
$MnSO_4$	28.66	151.01	0.95
Li_2SO_4	25.54	109.95	0.95
NaOH	12.74	40.00	0.97
Na_2CO_3	26.39	103.99	0.97
$(NH_4)_2SO_4$	31.01	132.29	0.86

that the salt phase is virtually free of PEG at long tie line lengths. This also means that the salting-out constant of the Setchenow equation (eq 3) is not a constant, indicating a change in activity coefficient over these extended tie line lengths. These data are not shown but may easily be calculated from Table 3.

$$\ln \frac{w_i^{\mathrm{T}}}{w_i^{\mathrm{B}}} = \beta_i + k_j^i(k_j^{\mathrm{B}} - w_j^{\mathrm{T}}) \tag{3}$$

In eq 3, w represents the mass concentrations of the two species i and j in the two phases, T and B. The k term is the salting-out coefficient, and β is a constant related to the activity coefficient.

We have also treated the data using an equation derived from statistical geometrical considerations by Lilley (eq 2). The results, which are given in Table 4, show the effective excluded volume (EEV or V^*, the fitted parameter of eq 2) and the regression coefficient. The latter indicates a rather poor fit from a practical point of view. However, the single fitted parameter should, at constant PEG molar mass, be related to the salting-out strength of the salt. Figure 10 shows the EEV in relation to the molar mass of the ABS phase-forming salts examined. It appears that there is a close relationship between the molar mass of the salt and its excluded volume. Unfortunately, this can only really be considered an artifact of the Lilley equation, since such a relationship cannot in general be true. Consider for instance the well-known exception in many attempts to correlate the Hofmeister series represented by $CaCl_2$

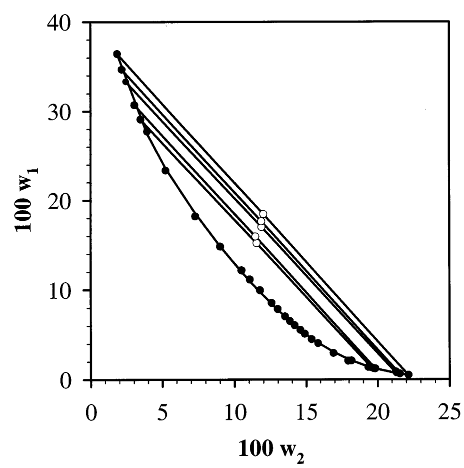

Figure 7. Phase diagram in w/w % of the PEG-2000 (1) + $MnSO_4$ (2) ABS, showing the binodal curve determined by cloud point titration (●), the fitted cloud point curve, and the overall and node compositions (○) of several fitted tie lines.

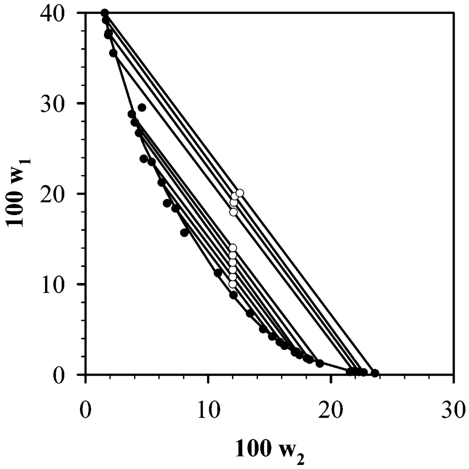

Figure 8. Phase diagram in w/w % of the PEG-2000 (1) + $ZnSO_4$ (2) ABS, showing the binodal curve determined by cloud point titration (●), the fitted cloud point curve, and the overall and node compositions (○) of several fitted tie lines.

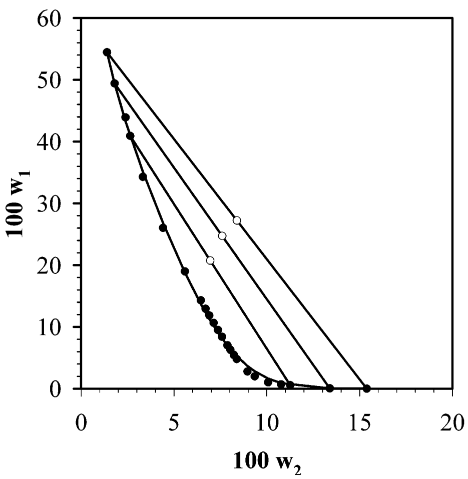

Figure 9. Phase diagram in w/w % of the PEG-2000 (1) + NaOH (2) ABS, showing the binodal curve determined by cloud point titration (●), the fitted cloud point curve, and the overall and node compositions (○) of several fitted tie lines.

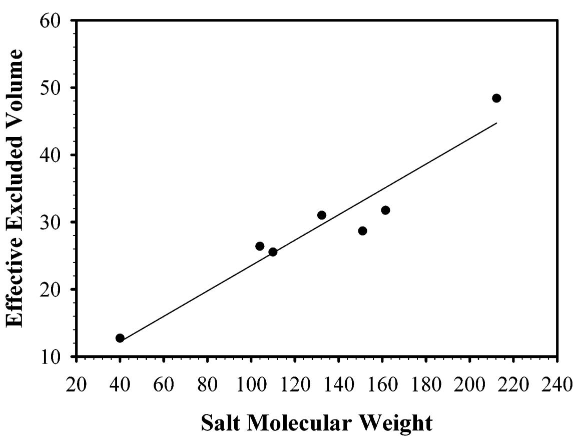

Figure 10. Effective excluded volume from Lilley's statistical geometry as determined for various PEG + salt ABS in relation to salt molecular size.

compared to NaCl, for example, in the treatment of protein precipitation by Mellander and Horvath[36] or in the depression of PEG cloud point temperature with salt concentration in the data reported by Bailey.[37]

Literature Cited

(1) Albertsson, P.-Å. *Partition of Cell Particles and Macromolecules*, 3rd ed.; Wiley: New York, 1986.
(2) Walter, H., Brooks, D. E., Fisher, D., Eds. *Partitioning in Aqueous Two-Phase Systems: Theory, Methods, Uses, and Applications to Biotechnology*; Academic Press: Orlando, FL, 1985.
(3) Fisher, D., Sutherland, I. A., Eds. *Separations using aqueous phase systems: applications in cell biology and biotechnology*; Plenum Press: New York, 1989.
(4) Zaslavsky, B. Y. *Aqueous Two-Phase Partitioning*; Marcel Dekker: New York, 1995.
(5) Walter, H., Johansson, G., Eds. *Aqueous Two-Phase Systems*; Methods in Enzymology, Vol. 228; Academic Press: New York, 1994.
(6) Hustedt, H.; Kroner, K.-H.; Kula, M.-R. Application of Phase Partitioning in Biotechnology. In *Partitioning in Aqueous Two-Phase Systems*; Walter, H., Brooks, D. E., Fisher, D., Eds.; Academic Press: New York, 1985; pp 529−587.
(7) Huddleston, J. G.; Veide, A.; Köhler, K.; Flanagan, J.; Enfors, S-O.; Lyddiatt, A. The Molecular Basis of Partitioning in Aqueous Two-Phase Systems. *Tibtech* **1991**, *9*, 381−388.
(8) Kula, M.-R.; Halfar, M.; Thommes, J. Primary recovery of a secreted recombinant human chymotrypsinogen B from Pichia pastoris culture broth: EBA vs. aqueous two-phase extraction. *Abstr. Pap. Am. Chem. Soc.* **2001**, 221: 69-BIOT Part 1.
(9) Tjerneld, F.; Persson, I.; Albertsson, P.-Å.; Hahn-Hägerdal, B. Enzymatic hydrolysis of cellulose in aqueous two-phase systems. II. Semi-continuous conversion of a model substrate. *Solka Floc BW 200. Biotechnol. Bioeng.* **1985**, *27*, 1044−1050.
(10) Andersson, E.; Hahn-Hägerdal, B. Bioconversions in aqueous two-phase systems. *Enzyme Microb. Technol.* **1990**, *12*, 242−254.
(11) Rogers, R. D.; Zhang, J. New Technologies for Metal Ion Separations Polyethylene Glycol Based-Aqueous Biphasic Systems and Aqueous Biphasic Extraction Chromatography. In *Ion Exchange and Solvent Extraction*; Marinsky, J. A., Marcus, Y., Eds.; Marcel Dekker: New York, 1997; Vol. 13, Chapter 4, pp 141−193.
(12) Huddleston, J. G.; Willauer, H. D.; Griffin, S. T.; Rogers, R. D. Aqueous Polymeric Solutions as Environmentally Benign Solvent Extraction Media. *Ind. Eng. Chem. Res.* **1999**, *38*, 2523−2539.
(13) Spear, S. K.; Griffin, S. T.; Huddleston, J. G.; Rogers, R. D. Radiopharmaceutical and Hydrometalllurgical Separations of Perrhenate Using Aqueous Biphasic Systems and the Analagous Aqueous Biphasic Extraction Chromatographic Resins. *Ind. Eng. Chem. Res.* **2000**, *39*, 3173−3180.
(14) Chaiko, D. J.; Mego, W. A. Method for Separating Water Soluble Organics from a Process Stream by Aqueous Biphasic Extraction. U.S. Patent 5 948 263, 1999.
(15) Willauer, H. D.; Huddleston, J. G.; Rogers, R. D. Solute Partitioning in Aqueous Biphasic Systems Composed of Polyethylene Glycol and Salt: The Partitioning of Small Neutral Organic Species. *Ind. Eng. Chem. Res.* **2002**, *41*, 1892−1904.
(16) Zhu, Z.; Guan, Y.; Li, M. Applications of Aqueous Two-phase Systems in Extraction and Synthesis of Antibiotics. *J. Chem. Ind. Eng.* **2001**, *52*, 1039−1048.
(17) Willauer, H. D.; Huddleston, J. G.; Rogers, R. D. Solvent Properties of Aqueous Biphasic Systems Composed of Polyethylene Glycol and Salt Characterized by the Free Energy of Transfer of a Methylene Group Between the Phases and by a Linear Solvation Energy Relationship. *Ind. Eng. Chem. Res.* **2002**, *41*, 2591−2601.
(18) Chaiko, D. J.; Mensah-Biney, R. Aqueous Biphasic Plutonium Oxide Extraction Process with pH and Particle Control, U. S. Patent 5 625 862, 1997.
(19) Willauer, H. D.; Huddleston, J. G.; Rogers, R. D. Aqueous Biphasic Systems for the Separation of Lignins from Cellulose in the Paper Pulping Process. *J. Chromatogr. B* **2000**, *743*, 127−135.
(20) Guo, Z.; Li, M.; Willauer, H. D.; Huddleston, J. G.; April, G. C.; Rogers, R. D. Evaluation of Polymer-Based Aqueous Biphasic Systems As Improvement for the Hardwood Alkaline Pulping Process. *Ind. Eng. Chem. Res.* **2002**, *41*, 2535−2542.
(21) Guo, Z.; Huddleston, J. G.; Rogers, R. D.; April, G. C. Reaction Parameter Effects on Metal Salt Catalyzed Aqueous Biphasic Pulping Systems. *Ind. Eng. Chem. Res.* **2003**, *42*, 248−253.
(22) Chen, J.; Spear, S. K.; Huddleston, J. G.; Holbrey, J. D.; Swatloski, R. P.; Rogers, R. D. Can polyethylene glycol based aqueous biphasic systems serve as green reaction and reactive extraction media? *Green Chem.* (Submitted).
(23) Lyddiatt, A. Process Chromatography: Current Constraints and Future Options for the Adsorptive Recovery of Bioproducts. *Curr. Opin. Biotechnol.* **2002**, *13*, 95−103.
(24) Meller da Silva, L. H.; Meirelles, A. J. A. PEG + Potassium Phosphate + Urea Aqueous Two-Phase Systems: Phase Equilibrium and Protein Partitioning, *J. Chem. Eng. Data* **2001**, *46*, 251−255.
(25) Grossman, C.; Tintinger, R.; Zhu, J.; Maurer, G. Partitioning of some amino acids and low molecular weight peptides in aqueous two-phase systems of poly(ethylene glycol) and dipotassium hydrogen phosphate. *Fluid Phase Equilib.* **1997**, *137*, 209−228.

(26) Salabat, A. The influence of salts on the phase composition in aqueous two-phase systems: experiments and predictions. *Fluid Phase Equilib.* **2001**, *187−188*, 487−498.

(27) Zafarani-Moattar, M. T.; Gasemi, J. Liquid−liquid equilibria of aqueous two-phase systems containing poly(ethylene glycol) and ammonium dihydrogen phosphate or diammonium hydrogen phosphate. Experiment and correlation. *Fluid Phase Equilib.* **2002**, *198*, 281−291.

(28) Grossman, C.; Tintinger, R.; Zhu, J.; Maurer, G. Aqueous Two Phase Systems of Poly(ethylene glycol) and dextran−experimental results and modeling of thermodynamic properties. *Fluid Phase Equilib.* **1995**, *106*, 111−138.

(29) Furuya, T.; Yamada, S.; Zhu, J.; Yamaguchi, Y.; Iwai, Y.; Arai, Y. Measurement and correlation of liquid−liquid equilibria and partition coefficients of hydrolytic enzymes for Dex T500 + PEG 20000 + water aqueous two-phase system at 20 °C. *Fluid Phase Equilib.* **1996**, *125*, 89−102.

(30) Grossmann, C.; Tintinger, R.; Jiandung, Z.; Maurer, G. Partitioning of Low Molecular Combination Peptides in Aqueous Two-Phase Systems of Poly(ethylene glycol) and Dextran in the Presence of Small Amounts of K_2HPO_4/KH_2PO_4 Buffer at 293 K: Experimental Results and Predictions. *Biotechnol. Bioeng.* **1998**, *60*, 699−711.

(31) Li, W.; Zhu, Z.-Q.; Li, M. Measurement and calculation of liquid−liquid equilibria of binary aqueous polymer solutions. *Chem. Eng. J.* **2000**, *78*, 179−185.

(32) Li, M.; Zhu, Z.-Q.; Wu, Y.-T.; Lin, D.-Q. Measurement of phase diagrams for new aqueous two-phase systems and prediction by a generalized multicomponent osmotic virial equation. *Chem. Eng. Sci.* **1998**, *53*, 2755−2767.

(33) Bamberger, S.; Brooks, D. E.; Sharp, K. A.; Van Alstine, J. M.; Webber, T. J. Prepartion of Phase Systems and Measurement of their Physicochemical Properties. In *Partitioning in Aqueous Two-Phase Systems: Theory, Methods, Uses, and Applications to Biotechnology*; Walter, H., Brooks, D. E., Fisher, D., Eds.; Academic Press: Orlando, FL, 1985.

(34) Merchuk, J. C.; Andrews, B. A.; Asenjo, J. A. Aqueous Two-Phase Systems for Protein Separation. Studies on Phase Inversion. *J. Chromatogr. B* **1998**, *711*, 285−293.

(35) Guan, Y.; Treffry, T. E.; Lilley, T. H. Application of a Statistical Geometrical Theory to Aqueous Two-Phase Systems. *J. Chromatogr. B* **1994**, *668*, 31−45.

(36) Melander, W.; Horvath, Cs. Salt Effects on Hydrophobic Interactions in Precipitation and Chromatography of Proteins: An Interpretation of the Lyotropic Series. *Arch. Biochem. Bipophys.* **1977**, *183*, 200−215.

(37) Bailey, F. E.; Koleske, J. V. *Alkylene Oxides and their Polymers*; Marcel Dekker: New York, 1991.

Received for review February 25, 2003. Accepted June 2, 2003. This research was supported by the Division of Chemical Sciences, Geosciences, and Biosciences, Office of Basic Energy Research, U.S. Department of Energy (Grant DE-FG02-96ER14673).

JE034042P